Spectra of Mo XXXI–XXXIV from exploded-Mo-wire plasmas

P. G. Burkhalter
Naval Research Laboratory, Washington, D.C. 20375

R. Schneider
Physics International Company, San Leandro, California 94577

C. M. Dozier
Naval Research Laboratory, Washington, D.C. 20375

Robert D. Cowan
University of California, Los Alamos Scientific Laboratory, Los Alamos, New Mexico 87545
(Received 4 January 1978)

The ionization stages in x-ray spectral data (3–5.5 Å) from single- and multiple-exploded-Mo-wire experiments were interpreted with atomic-structure calculations. Both exploded-wire experiments produced spectra in which Ne-like Mo XXXIII was the most abundant ionization stage. Experimental wavelengths from higher Rydberg transitions in Mo XXXIII were obtained. Except for the Ne-like lines, the Mo spectra are characterized by complex, overlapping line structure due to the F- and Na-like ionization stages.

I. INTRODUCTION

Molybdenum is one of the refractory metals used as a current limiter in tokamak generators. The radial distributions of Mo impurity ions in the Princeton ST and TFR (Tokamak Fontenay-aux-Roses) tokamaks were measured from intensity distributions of several xuv transitions believed to be in Na-like Mo XXXII and Mg-like Mo XXXI ions.[1,2] Recently, accurate wavelengths for transitions from Na- and Mg-like Mo ions were measured in both the 10-20-Å and 90-180-Å regions from a Nd:glass laser-produced spectrum[3]; and this work gave support to the identification of the lines in the tokamak plasmas as being from Mo ions. This same laser system located at the Naval Research Laboratory (NRL) produced plasmas hot enough to excite the Ne-like x-ray transitions as high in atomic number as Zr ($Z=40$).[4] The plasma generated by the focused, glass laser at the Lebedev Institute successfully excited Ne-like Mo XXXIII.[5] Wavelengths in the 4–5.5-Å x-ray region were reported for six $\Delta n=1$ resonance transitions to the $2s$ and $2p$ ground-state levels[5]; however, identification of the complex transitions in the ionization stages adjacent to Mo XXXIII was not attempted. Exploded wires provide a source of x-ray emission and are capable of producing highly ionized high-Z spectra.[6,7] The exploded-Mo-wire spectra are similar in appearance to the reported laser-produced Zr spectrum[4] in which the Na- and Mg-like satellite lines were identified. The purpose of the present work is to provide detailed interpretation of exploded-Mo-wire x-ray spectra in the 3–5.5-Å region. In addition to providing new wavelengths, the spectral data may be valuable for testing plasma models that can predict x-ray emission produced in hot, dense plasmas containing high-Z atoms.

II. EXPERIMENTAL

Two different exploded-wire generators provided the Mo spectra for this spectroscopic study. In the Gamble II generator at the NRL, a molybdenum spectrum was produced from a 25-μm-diam, single wire exploded at the 1-TW level. The spectrum was recorded with a 44-mm radius, convex curved-Potassium acid phthalate (KAP) crystal spectrograph. Details of the experimental arrangement are given in Ref. 7. In the Pithon generator at the Physics International Co., a symmetric array of six 12-μm-diam wires placed in a 1.5-cm-diam circle was exploded. The x-ray spectrograph was apertured to observe the plasma implosion generated at the center of the wire array with curved KAP and graphite crystals in a single spectrograph. The KAP crystal in the multiwire experiment was curved to a 16-mm radius. A small rotation of the spectrograph (crystal plus apertures) allowed collection of the second-order and (013) plane Mo spectrum in the multiwire experiment. In both experiments, the data were collected on Kodak No-Screen film in single shots. The spectra were scanned with a digitizing Grant densitometer. The densities were processed with a computer code to obtain spectral traces of the relative x-ray intensities. The spectral densities were corrected for filter absorption, film sensitivities using published data for No-Screen film,[8,9] and the crystal reflection coefficients for convex curved-KAP crystals.[10] Wavelength calibrations

were obtained from least-square fitting to the reported laser wavelength values for $\Delta n = 1$ transitions in Mo XXXIII in the 4.4–5.2-Å region and the location of the potassium-absorption edge (due to the KAP crystal) observed in the single-wire exposures. Wavelengths and oscillator strengths were calculated with an atomic-structure code written by one of us (R.D.C.). The spectra shown in this work are spatially and temporally integrated from the emission along a portion of the exploded wire or wire array.

III. RESULTS

A. Major series

Spectra from the single-Mo-wire and the multiwire array collected in first order with the KAP crystal spectrographs are shown in Fig. 1. The most distinct and intense lines in the exploded-wire x-ray spectra belong to Ne-like Mo XXXIII. The positions of the calculated wavelengths and their corresponding oscillator strengths (gf values) for Ne- and F-like transitions are plotted below each spectrum. The oscillator strengths, as indicated by the height of the lines in Fig. 1, have been scaled to most-intense $2p$-$3d$ line at 4.804 Å. The exploded-single-wire spectrum was recorded from a slightly hotter plasma than in the multiwire shot. A similar finding resulted from the comparison of other single- and multiwire spectra collected in another exploded-wire generator, OWL II.[11] In that study, for wires with Z between 13 and 26, slightly higher plasma temperatures were produced in the single-wire shots compared to the multiwire shots. The relative intensities for the distinct transitions in Mo XXXIV (e.g., the line at 4.502 Å) are higher in the single-wire spectrum. The wavelength and gf values for Mo XXXIII and XXXIV are duplicated for each spectrum except that the gf values for Mo XXXIV were scaled by 0.6 for the single-wire and by 0.4 for the multiwire shot to obtain a closer spectral match, reflecting some difference in the plasma temperature for the two experiments. The calculated wavelengths for the Ne-like transitions agree almost exactly with the wavelengths published for the $\Delta n = 1$ Ne-like transitions. The calculated F-like transitions show agreement with the experimental line structure between 4.3 and 4.6 Å. The spectral features with peaks at 4.664 and 4.691 Å are identified with the $2p$-$3d$ transitions in Mo XXXIV; however, as will be discussed later, wavelengths for transitions in lower stages of ionization overlap with the F-like transitions for these peaks.

In the single-wire spectrum, the inner-shell transitions $L\alpha_1$ and $L\beta_1$ are found. They are produced by energetic electrons. These inner-shell

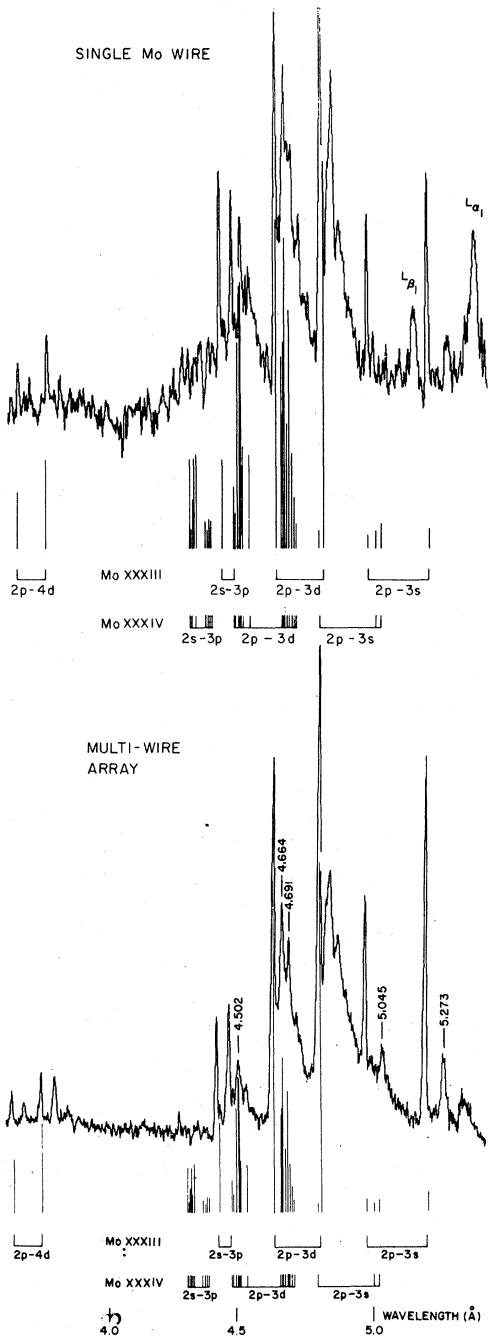

FIG. 1. Exploded-Mo-wire spectral intensities for single- and multiwire experiments and the calculated line structure for Ne- and F-like ionization stages. Both spectra were collected in first order with the KAP crystal spectrograph.

transitions are broader than the $2p$-$3s$ resonance lines and are shifted by 10 eV to shorter wavelengths than Mo $L\alpha_1$ and $L\beta_1$ transitions produced in cold target x-ray tubes. This energy shift corresponds to Mo ions with 12–13 outer electrons re-

moved as determined from Hartree-Fock-Slater calculations. A coronal-plasma temperature of 50–100 eV was estimated from an average ionization level of about 12 for the cool plasma regions that emit the $L\alpha_1$ and $L\beta_1$ lines. In a pinhole photograph for this single-wire shot, x-ray emission was observed from pinched spots (< 125-μm in diameter) colinear with the original wire position. Surrounding each pinch is a broader region of less intense x-ray emission believed to be the cool plasma. In the multiwire shots, the pinhole camera observes the plasma implosion formed at the center of the wire array. A pinhole photograph was not available for the Mo multiwire shot. A pinhole image of a multi-Ag-wire array revealed a more-uniform x-ray emission with a snakelike structure of about 400-μm width, similar to that observed for imploded plasma from Al-wire arrays.[12]

B. Satellites

Transitions in Mo XXXII and XXXI, with one or two $3s$, $3p$, or $3d$ electrons in the lower-level state, form satellite line structure on the long-wavelength side of the Ne-like resonance lines. The calculated satellite transitions for Na- and Mg-like Mo have wavelengths differing by 1 mÅ or less, thereby making the identification of individual lines impossible with the present spectral resolution. The calculated and experimental $2p$-$3d$ satellite structure is seen in Fig. 2. All the calculated transitions are to be compared with each spectrum. There is agreement in the experimental spectral peaks for both experiments. Generally, the calculated line structure agrees with the spectral observations. One can associate the experimental peaks with transitions calculated for either ionization stage. The most outstanding ambiguity in line identification occurs for the 4.664-Å line which has overlapping structure from the $2p^6\,3d$-$2p^5 3d^2$ transitions in Mo XXXII (Fig. 2) and the $2p^5$-$2p^4 3d$ transitions in Mo XXXIV (Fig. 1).

The $2p$-$3s$ satellite region was analyzed with hope to identify distinct lines for a possible plasma-temperature determination. The temperature dependence of certain dielectronic transitions that are satellite to the $2p^6\,{}^1S$-$2p^5 3s\,{}^1P$ transition have been calculated for Mo XXXII lines.[13] The spectrum from the multiwire shot between 5 and 5.5 Å is shown in Fig. 3. The gf values were multiplied by 0.4 and by 0.14 for Mo XXXII and Mo XXXI, respectively. Both were scaled to the intensity for the $2p$-$3s$ transition at 5.202 Å in this figure. Only about one-half of the calculated Mo XXXII transitions, those with the larger gf values, were plotted. The calculated wavelengths and classifications

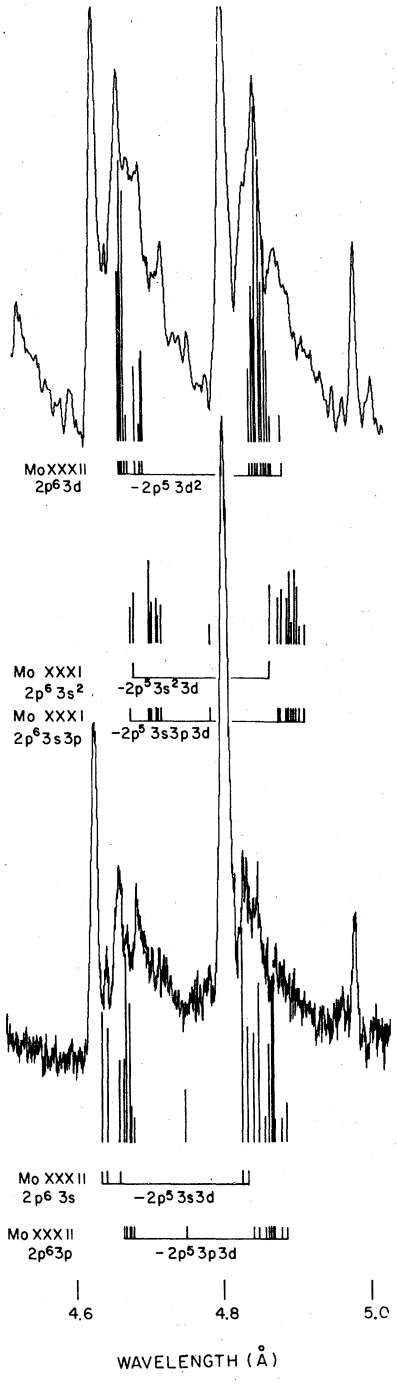

FIG. 2. Calculated $2p$-$3d$ satellite transitions plotted together with spectra from both experiments on a common wavelength scale. All the calculated transitions, plotted separately for the various configurations to avoid spectral overlap, are to be compared with each exploded-Mo-wire spectrum. The upper spectrum is an expanded view of the first-order single-wire shot while the lower one is the (013) plane spectrum collected with the KAP spectrograph for the multiwire shot.

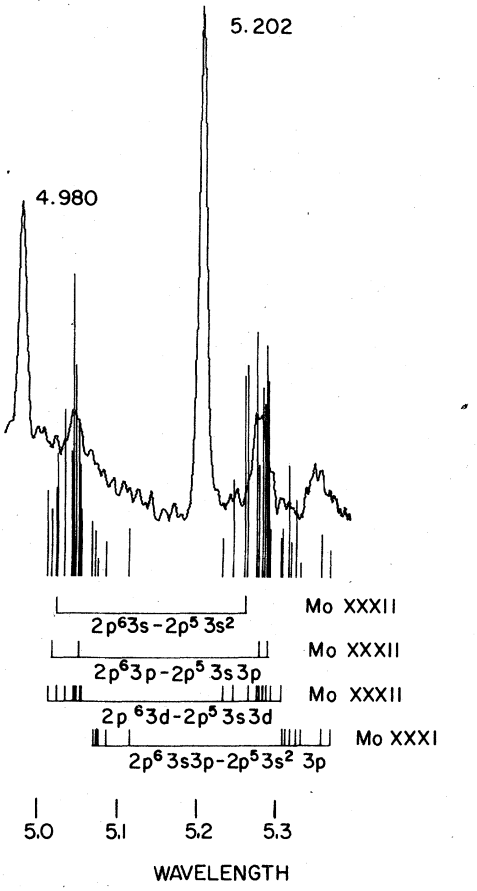

FIG. 3. Calculated $2p$-$3s$ satellite transitions near 5 Å compared with the multiwire spectrum.

in j-j coupling for the transitions plotted in Fig. 3 are listed in Table I. In this region, two intense satellite structures with peaks at 5.045 and 5.273 Å are found and have about the same wavelength separation as the $2p$-$3s$ resonance lines in Mo XXXIII. The two $2p^63s$-$2p^53s^2$ transitions in Mo XXXII have a calculated separation and relative gf values that would correspond to these two peaks. However, the calculated wavelengths for these two transitions are about 0.030 Å lower than the observed peaks. Also the line profiles of the satellite lines are broader than the resonance lines and therefore do not result from single transitions. The calculated wavelengths were shifted by +0.014 Å to achieve the spectral agreement between the calculated spectral pattern and the observed satellite structure in Fig. 3. The calculated wavelengths of many of the stronger transitions differ from each other by 0.002 Å or less and thus the satellites to the $2p$-$3s$ lines in Mo XXXIII form a complex, overlapping structure.

C. High Rydberg transitions

Transitions to higher Rydberg levels in Mo XXXIII were collected with the graphite crystal in the multiwire shots. Figure 4 shows the 3–4-Å Mo spectrum with the identification of the resonance lines based on the atomic-structure calculations. The calculated wavelengths were shifted by about 0.030 Å to larger wavelengths to obtain agreement with the observed line pattern. The broader lines at larger wavelengths, with approximately the same spacings as the corresponding resonance lines in the $2p$-$4d$, $5d$ regions, are assumed to be satellite line arrays similar to those identified in the $2p$-$3d$ region. No lines were observed above the weak continuum with wavelengths less than for the $2p$-$7d$ transitions. The wavelength values determined for the higher Rydberg transitions in Mo XXXIII are given in Table II. The energy calibration depended on the location of the potassium-absorption edge. The agreement between the experimental and calculated wavelengths is 0.03–0.04 Å which is about the uncertainty in the position of the absorption edge. The experimental wavelength values for the transitions to the higher Rydberg states ($n \geq 4$) were also found to be larger by 0.01 to 0.04 Å than wavelengths computed by a fully relativistic Dirac-Hartree-Fock code due to Desclaux.[14] The higher Rydberg transitions were not observable in the single-wire spectrum. There was less absorption material placed in front of the spectrograph for the Gamble II experiment, which allowed a higher level of low-energy radiation (< 1 keV) to scatter from the crystal at low angles and obscure the weak spectral lines below 3.5 Å.

IV. DISCUSSION

The Mo spectra produced from single- and multi-exploded wires have been interpreted by comparing them with atomic-structure calculations. The x-ray spectra from the individual exploded wires and the imploded plasmas from wire arrays have Ne-like Mo XXXIII as the most-abundant ionization stage. Agreement within 0.04 Å was found between the calculated and measured wavelengths in the Mo XXXIII transitions to high Rydberg states. The Ne-like transitions are observed to the $7p$ level in the multiwire data. The good agreement between the calculated transitions for F-, Na-, and Mg-like ions and the observed spectral patterns in the vicinity of the $2p$-$3d$ lines in Mo XXXIII identify the ionization stages in the exploded-wire spectra. Compared to the multiwire data, the distribution of ionization stages from Mo XXXI to Mo XXXIV in the single-wire data are shifted towards higher-

TABLE I. Calculated satellite transitions in Mo XXXII and Mo XXXI.

Calculated λ (Å)	gf	J [a]	J' [a]	E' [a] (cm^{-1})	Transition and composition of upper level [b,c] (j-j coupling)
				$2p^6 3s$-$2p^5 3s^2$	
5.012	0.069	$\frac{1}{2}$	$\frac{1}{2}$	19 954 000	$1.0(^2P_{1/2}, ^1S_0)$
5.247	0.111	$\frac{1}{2}$	$\frac{3}{2}$	19 059 000	$1.0(^2P_{3/2}, ^1S_0)$
				$2p^6 3p$-$2p^5 3p 3s$	
5.005	0.038	$\frac{1}{2}$	$\frac{1}{2}$	19 837 000	$0.80(^2P_{1/2}, ^2P_{1/2}, ^2S_{1/2})$ $0.15(^2P_{1/2}, ^2P_{3/2}, ^2S_{1/2})$
5.038	0.085	$\frac{1}{2}$	$\frac{3}{2}$	19 705 000	$0.92(^2P_{1/2}, ^2P_{1/2}, ^2S_{1/2})$
5.269	0.062	$\frac{1}{2}$	$\frac{1}{2}$	18 834 000	$0.95(^2P_{3/2}, ^2P_{1/2}, ^2S_{1/2})$
5.274	0.128	$\frac{1}{2}$	$\frac{3}{2}$	18 815 000	$0.77(^2P_{3/2}, ^2P_{1/2}, ^2S_{1/2})$ $0.14(^2P_{3/2}, ^2P_{1/2}, ^2S_{1/2})$
				$2p^6 3d$-$2p^5 3d 3s$	
5.002	0.049	$\frac{3}{2}$	$\frac{3}{2}$	19 965 000	$0.68(^2P_{1/2}, ^2D_{3/2}, ^2S_{1/2})$ $0.30(^2P_{1/2}, ^2D_{5/2}, ^2S_{1/2})$
5.013	0.050	$\frac{3}{2}$	$\frac{1}{2}$	19 920 000	$0.98(^2P_{1/2}, ^2D_{3/2}, ^2S_{1/2})$
5.021	0.093	$\frac{5}{2}$	$\frac{5}{2}$	19 936 000	$0.82(^2P_{1/2}, ^2D_{5/2}, ^2S_{1/2})$ $0.13(^2P_{1/2}, ^2D_{3/2}, ^2S_{1/2})$
5.032	0.069	$\frac{5}{2}$	$\frac{3}{2}$	19 892 000	$0.68(^2P_{1/2}, ^2D_{5/2}, ^2S_{1/2})$ $0.30(^2P_{1/2}, ^2D_{3/2}, ^2S_{1/2})$
5.034	0.167	$\frac{5}{2}$	$\frac{7}{2}$	19 882 000	$1.0(^2P_{1/2}, ^2D_{5/2}, ^2S_{1/2})$
5.036	0.116	$\frac{3}{2}$	$\frac{5}{2}$	19 830 000	$0.86(^2P_{1/2}, ^2D_{3/2}, ^2S_{1/2})$ $0.14(^2P_{1/2}, ^2D_{5/2}, ^2S_{1/2})$
5.040	0.063	$\frac{5}{2}$	$\frac{5}{2}$	19 861 000	$0.95(^2P_{1/2}, ^2D_{5/2}, ^2S_{1/2})$
5.231	0.054	$\frac{5}{2}$	$\frac{3}{2}$	19 137 000	$0.78(^2P_{3/2}, ^2D_{5/2}, ^2S_{1/2})$ $0.18(^2P_{3/2}, ^2D_{3/2}, ^2S_{1/2})$
5.250	0.119	$\frac{5}{2}$	$\frac{5}{2}$	19 067 000	$0.86(^2P_{3/2}, ^2D_{5/2}, ^2S_{1/2})$ $0.10(^2P_{3/2}, ^2D_{3/2}, ^2S_{1/2})$
5.261	0.136	$\frac{5}{2}$	$\frac{7}{2}$	19 027 000	$0.78(^2P_{3/2}, ^2D_{5/2}, ^2S_{1/2})$ $0.17(^2P_{3/2}, ^2D_{3/2}, ^2S_{1/2})$
5.263	0.844	$\frac{5}{2}$	$\frac{3}{2}$	19 020 000	$0.90(^2P_{3/2}, ^2D_{5/2}, ^2S_{1/2})$
5.267	0.115	$\frac{3}{2}$	$\frac{3}{2}$	18 959 000	$0.89(^2P_{3/2}, ^2D_{3/2}, ^2S_{1/2})$
5.267	0.104	$\frac{5}{2}$	$\frac{7}{2}$	19 004 000	$0.93(^2P_{3/2}, ^2D_{5/2}, ^2S_{1/2})$
5.269	0.062	$\frac{3}{2}$	$\frac{1}{2}$	18 949 000	$0.75(^2P_{3/2}, ^2D_{3/2}, ^2S_{1/2})$ $0.23(^2P_{3/2}, ^2D_{3/2}, ^2S_{1/2})$
5.270	0.129	$\frac{3}{2}$	$\frac{5}{2}$	18 947 000	$0.45(^2P_{3/2}, ^2D_{3/2}, ^2S_{1/2})$ $0.29(^2P_{3/2}, ^2D_{5/2}, ^2S_{1/2})$
5.272	0.096	$\frac{5}{2}$	$\frac{5}{2}$	18 989 000	$0.63(^2P_{3/2}, ^2D_{5/2}, ^2S_{1/2})$ $0.23(^2P_{3/2}, ^2D_{3/2}, ^2S_{1/2})$
5.276	0.034	$\frac{3}{2}$	$\frac{5}{2}$	18 925 000	$0.49(^2P_{3/2}, ^2D_{3/2}, ^2S_{1/2})$ $0.44(^2P_{3/2}, ^2D_{3/2}, ^2S_{1/2})$
				$2p^6 3s 3p$-$2p^5 3s^2 3p$	
5.057	0.089	2	2	19 793 000	$1.0(^2P_{1/2}, ^1S_0, ^2P_{3/2})$
5.060	0.082	2	1	19 783 000	$1.0(^2P_{3/2}, ^1S_0, ^2P_{3/2})$
5.061	0.033	0	1	19 567 000	$1.0(^2P_{1/2}, ^1S_0, ^2P_{1/2})$
5.071	0.054	1	1	19 567 000	$1.0(^2P_{1/2}, ^1S_0, ^2P_{1/2})$
5.101	0.079	1	2	19 793 000	$1.0(^2P_{1/2}, ^1S_0, ^2P_{3/2})$
5.291	0.077	2	2	18 920 000	$1.0(^2P_{3/2}, ^1S_0, ^2P_{3/2})$
5.301	0.182	2	3	18 883 000	$1.0(^2P_{3/2}, ^1S_0, ^2P_{3/2})$
5.302	0.053	0	1	18 669 000	$0.97(^2P_{3/2}, ^1S_0, ^2P_{1/2})$
5.308	0.127	1	2	18 685 000	$1.0(^2P_{3/2}, ^1S_0, ^2P_{1/2})$

TABLE I. (*Continued*)

Calculated λ (A)	gf	J [a]	J' [a]	E' [a] (cm^{-1})	Transition and composition of upper level [b,c] (j-j coupling)
5.313	0.025	1	1	18 669 000	$0.97(^2P_{3/2}, ^1S_0, ^2P_{1/2})$
5.338	0.066	1	2	18 920 000	$1.0(^2P_{3/2}, ^1S_0, ^2P_{3/2})$
5.348	0.043	1	1	18 886 000	$0.97(^2P_{3/2}, ^1S_0, ^2P_{3/2})$

[a] The symbols J and J' represent the total angular momentum of the lower and upper levels, respectively. The symbol E' is the theoretical eigenvalue of the upper configuration.

[b] The square of the eigenfunction components are listed, and only if greater than 0.1 in magnitude.

[c] Abbreviated notation $(^2P_{1/2}, ^1S_0)$ in place of $(2p^5\,^2P_{1/2}, 3s^2\,^1S_0)$.

ionization stages. In the single-wire spectrum, inner-shell transitions are produced in cool-plasma regions. If these transitions are produced in the multiwire implosions, their emission is much weaker than from single wires.

Various plasma models could be used for temperature estimates from the distribution of ionization stages in the exploded-wire spectra. However, a plasma model for the hot, dense exploded-Mo-wire sources is not available. Densities of 10^{20} to 10^{21} e/cm^3 have been determined for exploded-Al-wire plasmas.[11] For low-density hot plasmas, such as are found in tokamaks, the coronal model yields plasma temperatures that are in general agreement with those determined by Thomson scattering. xuv transitions in Na- and Mg-like Mo are observed when the tokamak plasma temperatures (determined by Thomson scattering) are between 1.5 and 2.0 keV, which agrees with coronal calculations that include dielectronic recombination.[15,16] Both the normal coronal models[15] and the coronal model based on the average atom configuration[16] predict that a 3–4-keV plasma temperature corresponds to high abundances of Ne- and F-like ions. Plasma temperatures of 3.6 and 4.2 keV were estimated for the multiwire and single wire spectra, respectively, from the observed abundances of ionization stages. These estimates were determined from coronal-model calculations[15] for low-density plasmas ($<10^{16}e/cm^3$). The exploded-Mo-wire conditions are near the coronal limit and significant changes in the temperatures derived from the data are not anticipated as other plasma models become available for Mo.

Another method for estimating temperatures in Mo plasmas uses the ratio of satellite-to-parent-line intensities in Mo XXXII and Mo XXXIII. Such calculations have been made for Mo based on coronal equilibrium.[13] The spectral complexity of the $2p$-$3s$ satellite at the present dispersion level did not allow an exact temperature estimate for the recombining plasma. However, assuming that a portion of the peak of the satellite line at 5.045 Å corresponds to the most-intense dielectronic transition ($2p^6 3d$-$2p^5 3s 3d$ in Mo XXXII), the experimental intensity ratio of this satellite peak to the Ne-like resonance line gave an approximate temperature range of 2.5–3 keV.

The question arises as to whether x-ray crystals are available to separate the satellite transitions

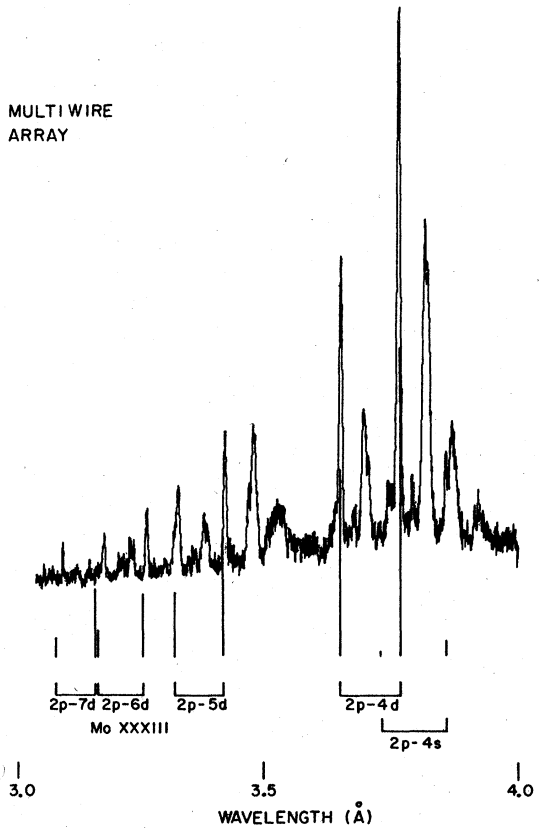

FIG. 4. Calculated high Rydberg transitions in Ne-like Mo compared with the short-wavelength multiwire spectrum.

TABLE II. Experimental and calculated values for transitions in Mo XXXIII.

Experimental λ (Å)	Int.		Calculated λ (Å)	gf	Classification in j-j coupling
5.202 [a]	50 [b]	85 [c]	5.203	0.11	$2p^6-[2p^5(^2P_{3/2}),3s]_1$
4.980 [a]	40	40	4.974	0.07	$2p^6-[2p^5(^2P_{1/2}),3s]_1$
			4.856	0.00	$2p^6-[2p^5(^2P_{3/2}),3d(^2D_{3/2})]_1$
4.804 [a]	100	100	4.804	1.9	$2p^6-[2p^5(^2P_{3/2}),3d(^2D_{5/2})]_1$
4.630 [a]	90	85	4.625	1.7	$2p^6-[2p^5(^2P_{1/2}),3d(^2D_{3/2})]_1$
4.464 [a]	35	30	4.465	0.17	$2s^22p^6-[2s2p^63p(^2P_{1/2})]_1$
4.416 [a]	45	30	4.417	0.46	$2s^22p^6-[2s2p^63p(^2P_{3/2})]_1$
3.85	3	2	3.828	0.022	$2p^6-[2p^5(^2P_{3/2}),4s]_1$
3.76	19	12	3.739	0.461	$2p^6-[2p^5(^2P_{3/2}),4d(^2D_{5/2})]_1$
3.74	1.5	1.2	3.701	0.008	$2p^6-[2p^5(^2P_{1/2}),4s]_1$
3.64	12	7	3.622	0.280	$2p^6-[2p^5(^2P_{1/2}),4d(^2D_{3/2})]_1$
3.42		3.5	3.391	0.179	$2p^6-[2p^5(^2P_{3/2}),5d(^2D_{5/2})]_1$
3.32		2.3	3.293	0.098	$2p^6-[2p^5(^2P_{1/2}),5d(^2D_{3/2})]_1$
3.26		1.8	3.228	0.096	$2p^6-[2p^5(^2P_{3/2}),6d(^2D_{5/2})]_1$
3.18		1.1	3.138	0.004	$2p^6-[2p^5(^2P_{1/2}),6d(^2D_{3/2})]_1$
			3.137	0.101	$2p^6-[2p^5(^2P_{3/2}),7d(^2D_{5/2})]_1$
3.09		0.8	3.052	0.029	$2p^6-[2p^5(^2P_{1/2}),7d(^2D_{3/2})]_1$

[a] Experimental wavelengths from laser data of Aglitskii *et al.* (Ref. 5).
[b] Single-exploded-Mo wire.
[c] Exploded-wire array.

in Mo spectra in order to obtain a more-precise plasma temperature. The linewidths for the $2p$-$3s$ resonance lines in MoXXXIII were 0.010 Å for the first-order KAP data. The dispersion for the Mo spectrum diffracted from the (013) plane in KAP ($2d = 8.06$ Å) was a factor-of-5 better. The dispersion was further improved for the Mo spectrum collected with the graphite crystal ($2d = 6.69$ Å) in the $2p$-$3d$ spectral region around 4.8 Å. However, no significant improvement in resolution was obtained because of line broadening introduced by the graphite crystal. In order to obtain separated satellite line structure, Mo spectral data should be collected with more-optimum $2d$-spacing diffraction crystals. But the diffraction efficiency of crystals and whether or not the crystal can be satisfactorily curved are also important in the crystal selection for a particular experiment. The use of a NaCl ($2d = 5.64$ Å) crystal to collect satellite data around 5.3 Å would improve the resolving power by an estimated order of magnitude and thereby provide resolved-satellite transitions. Other possible crystal choices include Si ($2d = 6.26$ Å) and the (014) plane in KAP ($2d = 6.29$ Å).

ACKNOWLEDGMENTS

We wish to thank L. Roszman of the National Bureau of Standards for a preprint of his intensity distribution for satellites in MoXXXII. The authors also express graditude to R. Whitlock of the X-Ray Optics Branch at the Naval Research Laboratory for the use of his computer code to obtain spectral intensity traces and to D. Brown for considering the (013) diffraction plane in KAP crystals. This work was supported by the Magnetic Fusion Energy Division of the U. S. Energy Research and Development Administration and by the Defense Nuclear Agency.

[1]Tokamak Fontenay-aux-Roses (TFR) Group, Nucl. Fusion 15, 1053–1066 (1975).
[2]E. Hinnov, Phys. Rev. A 14, 1533–1541 (1976).
[3]P. G. Burkhalter, Joseph Reader, and Robert D. Cowan, J. Opt. Soc. Am. 67, 1521–1525 (1977).
[4]P. G. Burkhalter, D. J. Nagel, and Robert D. Cowan, Phys. Rev. A 11, 782–788 (1975).
[5]E. V. Aglitskii, V. A. Boiko, O. N. Krokhin, S. A. Pikuz, and A. Ya. Faenov, Quantum Electron. 1, 2067–2069 (1974).
[6]C. M. Dozier, P. G. Burkhalter, D. J. Nagel, S. J. Stephanakis, and D. Mosher, J. Phys. B 10, L73–L77 (1977).
[7]P. G. Burkhalter, C. M. Dozier, and D. J. Nagel, Phys. Rev. A 15, 700–717 (1977).
[8]C. M. Dozier, D. B. Brown, L. S. Birks, P. B. Lyons and R. F. Benjamin, J. Appl. Phys. 47, 3732–3739 (1976).
[9]D. B. Brown, J. W. Criss, and L. S. Birks, J. Appl. Phys. 47, 3722–3731 (1976).
[10]D. B. Brown (unpublished).
[11]P. G. Burkhalter, J. Davis, and R. Schneider, (unpublished).
[12]C. Stallings, K. Nielsen, and R. Schneider, Appl. Phys. Lett. 29, 404–406 (1976).
[13]L. J. Roszman, Bull. Am. Phys. Soc. 21, 1118 (1976).
[14]J. P. Desclaux, Comput. Phys. Commun. 9, 31–45 (1975).
[15]C. Breton, C. de Michelis, and M. Mattioli, J. Quant. Spectrosc. Radiat. Transfer 19, 367–379 (1978).
[16]D. E. Post, R. V. Jensen, C. B. Tarter, W. H. Grasberger, and W. A. Lokke Princeton Plasma Physics Laboratory-1352, 1977 (unpublished), p. 87.